MESOPOROUS CERIA-SILICA COMPOSITES AS CARRIERS FOR DOXYCYCLINE

Marilena PETRESCU[1], Raul-Augustin MITRAN[2]*, Ana-Maria LUCHIAN[3], Cristian MATEI[4], Daniela BERGER[5]

Two synthesis strategies for obtaining ceria-silica mesoporous carriers for drug delivery applications were explored. Core-shell and MCM-CeO_2 composite materials were obtained by coating ceria nanoparticles with mesoporous silica and by one-step approach, respectively. Doxycycline was adsorbed onto the ceria-silica and MCM-41 silica carriers and the resulting hybrid samples and the inorganic supports were characterized by small- and wide-angle XRD, N_2 adsorption-desorption isotherms, FT-IR spectroscopy, and scanning electron microscopy. In vitro doxycycline release profiles were determined in phosphate buffer solution, pH 5.5, by UV-VIS spectroscopy. The MCM-CeO_2 composite containing 10% ceria nanoparticles exhibited the slowest antibiotic release rate, being the best doxycycline delivery support.

Keywords: doxycycline, drug-delivery systems, ceria, mesoporous silica, ceria-silica composite

1. Introduction

Recently, ceria-based composite materials and nanomaterials have received extensive attention due to their use in different fields such as catalysis [1], optical and luminescence applications [2], fuel cell technologies [3], gas sensors[4], solid state electrolytes [5] and medicine [6]. Nanoceria manifests a biologic potential by protecting cellular environment from reactive species damage in diseases associated with neuronal degeneration, having a high affinity for plasmatic membranes [7]. The antioxidant properties of ceria-based materials arise due to easy switching between +3 and +4 oxidation states of cerium ions.

[1] PhD Student, Dept. of Inorganic Chemistry, Physical Chemistry and Electrochemistry, University POLITEHNICA of Bucharest, Romania
[2] PhD Eng., Dept. of Inorganic Chemistry, Physical Chemistry and Electrochemistry, University POLITEHNICA of Bucharest, Romania, e-mail: raul.mitran@gmail.com
[3] Student, Dept. of Inorganic Chemistry, Physical Chemistry and Electrochemistry, University POLITEHNICA of Bucharest, Romania
[4] Prof., Dept. of Inorganic Chemistry, Physical Chemistry and Electrochemistry, University POLITEHNICA of Bucharest, Romania
[5] Prof., Dept. of Inorganic Chemistry, Physical Chemistry and Electrochemistry, University POLITEHNICA of Bucharest, Romania

An emerging class of materials for drug delivery applications is represented by mesostructured silica and aluminosilicate nanoparticles, which possess high porosity, ordered pore array, good biocompatibility and adsorption properties [8,9]. As a platform for drug delivery, mesoporous silica can be combined with inorganic or organic species, in order to create advanced composite materials with magnetic [10], stimuli-responsive properties [11], targeted or controlled delivery of biologically active molecules [12, 13]. To the best of our knowledge, ceria-silica mesoporous composites have not been previously investigated in drug delivery applications.

Doxycycline (scheme 1), which belongs to tetracycline class, developed by Pfizer in 1966 as a semi-synthetic and long-acting tetracycline, was employed as a model drug. Doxycycline is a broad-spectrum bacteriostatic antibiotic, inhibiting the elongation step of protein synthesis by blocking the binding of aminoacyl-tRNA to the small ribosomal subunit [14]. In addition to bacteriostatic properties, doxycycline shows anti-inflammatory, cytostatic and antiproliferative properties in various cancer cell lines [15, 16]. Its chemical structure makes it five to ten times more lipophilic and more plasma bound compared to its natural analogue tetracycline [17].

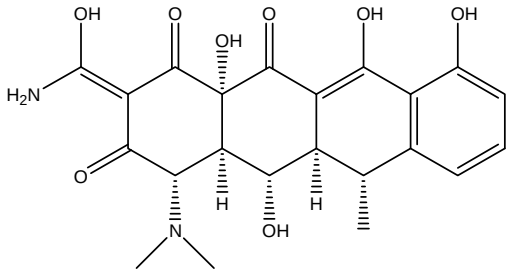

Scheme 1. The chemical structure of doxycycline

Herein we report the synthesis of novel ceria-silica mesoporous composites and the first experimental study on doxycycline adsorption and *in vitro* release using mesoporous ceria-silica and MCM-41 silica nanomaterials as drug carriers.

2. Experimental

2.1. Materials

Mesoporous MCM-41 silica (Aldrich), tetratethyl orthosilicate (TEOS, Fluka), trimethylhexadecylammonium bromide (CTAB, AlfaAesar), ammonia solution 25% (Scharlau), doxycycline hyclate (Doxy, Sigma-Aldrich), cerium (III) chloride heptahydrate (Sigma-Aldrich), ammonium cerium (IV) nitrate (Sigma-Aldrich) and solvents (Fluka) were used as purchased, without further

purification. Ultrapure deionized water (MilliQ water systems with Biopack UF cartridge) was used for all solutions and experiments.

2.2. Synthesis of CeO_2 nanoparticles (CeO_2 NP)

CeO_2 NP has been obtained by hydrothermal method, in the presence CTAB. 4 mL 25% ammonia aqueous solution were added to the previously prepared solution of CTAB by dissolution of 0.6 g CTAB in 30 mL water, followed by the dropwise addition of a 0.5 M $CeCl_3$ aqueous solution, the $CeCl_3$/CTAB molar ratio being 6.67. The reaction mixture was aged under magnetic stirring at 40 °C for 1 h and then was hydrothermally treated at 110 °C for 24 h. The solid was recovered by centrifugation and washed with hot water and ethanol.

2.3. Synthesis of CeO_2 core- MCM-41 silica shell nanoparticles (CeO_2@MCM-41)

Ceria nanoparticles (CeO_2 NP) previously obtained were dispersed into an aqueous CTAB solution, followed by the addition of 25% aqueous ammonia solution and TEOS, the TEOS /CeO_2 molar ratio being 19. The reaction mixture was magnetically stirred at 40 °C for 24 h and then was hydrothermal treated at 120 °C for 48 h. The solid was filtered off and intensively washed with hot water and ethanol. To remove completely the structure directing agent, the sample was calcined at 550 °C for 5 h.

2.4. Synthesis of MCM-CeO_2 composite

Ceria-silica composite were prepared by sol-gel method using TEOS as silicon precursor and cerium ammonium nitrate as cerium source, as well as CTAB as structure directing agent. To the solution containing CTAB, concentrated ammonia aqueous solution and TEOS were added. After TEOS precipitation at room temperature, aqueous solution of cerium ammonium nitrate was added. A molar ratio, TEOS : $(NH_4)_2Ce(NO_3)_6$: CTAB : NH_3, 1: 0.1: 0.25: 3.37, was employed. The reaction mixture was ageing under magnetic stirring for1h at 60°C for a good impregnation of colloidal silica precipitate with cerium cations. A hydrothermal treatment at 100 °C, 96 h was applied to the reaction mixture.

2.5. Doxycycline loading and in vitro release studies

Drug loading was performed by the incipient wetness impregnation technique according to a previously developed protocol [18, 19]. Typically, 50 mg

support was added to 0.5 mL doxycycline hyclate aqueous solution, which has 100 mg/mL concentration, gently stirred and dried under vacuum in dark conditions, at room temperature overnight. The hybrid materials are denoted "*doxy/support*".

In vitro drug release experiments were performed using a light-sealed reactor, at 37 °C, phosphate buffer solution (PBS, *p*H 5.5) as stimulated body fluid and a magnetic stirring rate of 150 rpm. An amount of drug loaded hybrid containing 10 mg doxycycline hyclate was dispersed into 100 mL PBS. Aliquots were periodically withdrawn, centrifuged, properly diluted and analyzed by UV-VIS spectroscopy. Drug concentration was computed using a previously obtained absorbance-concentration linear calibration curve.

2.6. Characterization

Both the carriers and drug-loaded materials were characterized by small- and wide-angle X-ray powder diffraction (XRD, Rigaku MiniFlex II diffractometer with CuKα radiation), FTIR spectroscopy (Bruker Tensor 27), scanning electron microscopy (SEM, Tescan Vega 3 LM) and nitrogen adsorption-desorption isotherms (Quantachrome Autosorb iQ_2) performed at 77 K. Specific surface area values (S_{BET})were determined using the Brunauer–Emmett–Teller model in the 0.05-0.3 relative pressure range of the adsorption isotherm, while the pore size distribution for the prepared materials was computed from the desorption branch employing the Barrett-Joyner-Halenda (BJH) theory. UV-VIS spectroscopy was carried out on an Ocean Optics USB 4000 spectrometer.

3. Results and discussion

3.1. Carrier synthesis and characterization

The formation of a crystalline cubic fluorite CeO_2 phase in all materials was evidenced by wide-angle XRD (Fig**. 1**). An amorphous silica phase is present in the core-shell (Fig**. 1**b) and composite materials (Fig**. 1** C), as demonstrated by the specific broad diffraction peak between 15-30°. Furthermore, the intensity of the CeO_2 peaks is reduced for the CeO_2@MCM-41, MCM-CeO_2 materials with respect to CeO_2 NP, as expected from the weight fraction decrease of the ceria cubic phase in these composite materials.

The small-angle XRD data (Fig**. 1**, inset) demonstrate that both core-shell and ceria-silica composite materials present ordered mesopore arrays, with at least one low-angle (10) Bragg reflection. The most ordered material, presenting three (10), (11) and (20) Bragg reflections characteristic for two-dimensional hexagonal *p6m* space group symmetry, is MCM-CeO_2.

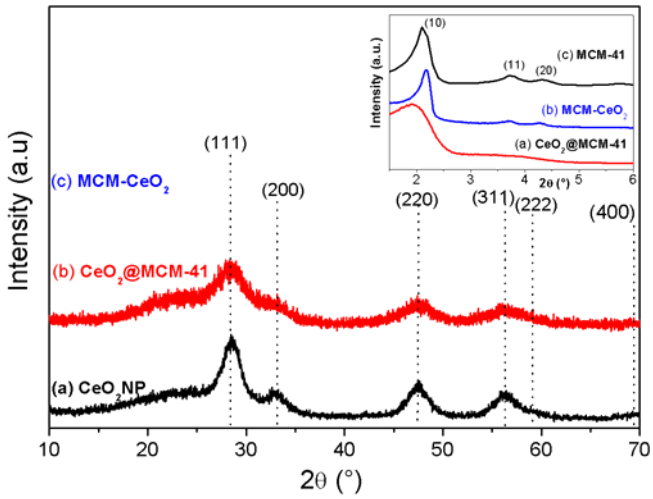

Fig. 1. Wide-angle XRD patterns of CeO_2-based carriers. Inset shows the small-angle XRD patterns of CeO_2-based carriers in comparison with MCM-41

CeO_2 sample consists of ~20 nm monodispersed nanoparticles (Fig. 2 A). Both the core-shell and ceria-silica composite materials are composed of aggregates of polydisperse spherical nanoparticles, typical of MCM-41 materials (Fig. 2 B and C). The SEM investigations of CeO_2@MCM-41 (Fig. 2 B) reveals that the ceria nanoparticles are dispersed inside the silica material.

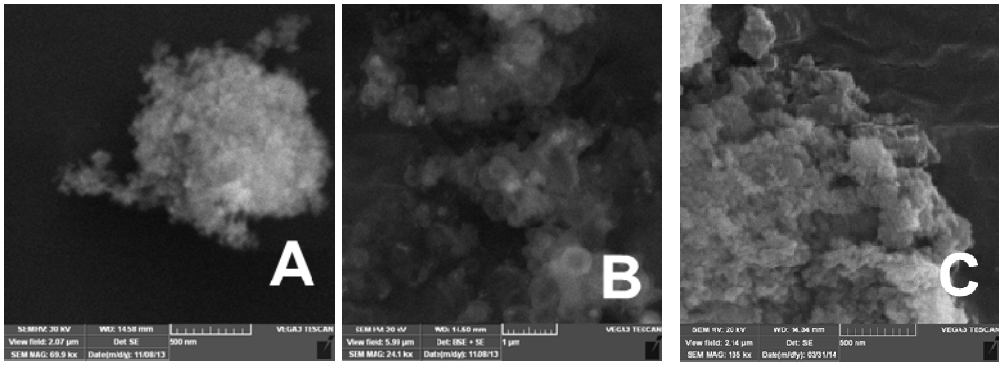

Fig. 2. SEM micrographs of CeO_2 NP (A), CeO_2@MCM-41(B) and MCM-CeO_2 (C)

The N_2 adsorption-desorption isotherm of CeO_2 NP (Fig. 3A curve a) is a type II isotherm, characteristic for non-porous materials, the BET specific surface area being 88 m^2/g. The CeO_2@MCM-41 and CeO_2-MCM samples present type IV isotherms, typical for mesoporous materials (Fig. 3A curves b and c). The core-shell CeO_2@MCM-41 material has a mesopore distribution between 2.6 and 3.8 nm, while the CeO_2-MCM sample has a monodispersed pore size distribution centered at 2.7 nm (Fig. 3B).

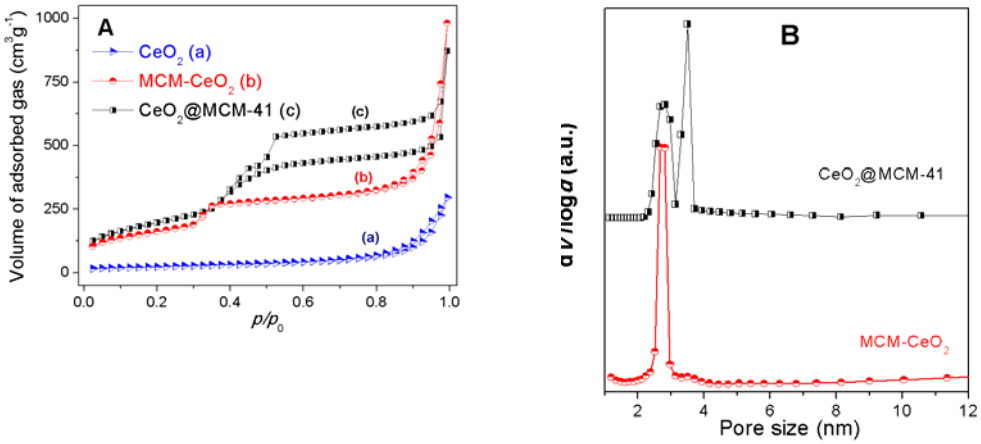

Fig. 3. N_2 adsorption-desorption isotherms of: CeO_2@MCM-41 (a), ceria-silica composite (b) and CeO_2 NP (c)

The capillary nitrogen condensation into mesoporous channels, occurring at ~ 0.42 relative pressure, results in a false peak in the BJH pore size distribution [20] at 4.0 nm. In comparison with MCM-41 mesoporous silica, with average pore size, d_{BJH}, of about 3.0 nm, the core-shell material has larger pores (3.3 nm), while the MCM-CeO_2 carrier have slightly lower pore sizes (2.7 nm) (*Table 1*).

Table 1

Textural parameters of mesoporous carriers and doxycycline loaded hybrids

Sample	**Doxycycline content in hybrids (%)**	**d_{BJH} (nm)**	**S_{BET} (m^2g^{-1})**	**$V_{mesopore}$ (cm^3g^{-1})**
MCM-41	-	3.0	959	0.91
CeO_2 NP	-	-	88	0.10
CeO_2@MCM-41	-	3.3	717	1.40
MCM- CeO_2	-	2.7	683	0.67
Doxy/CeO_2@MCM-41	25	3.2	266	0.61
Doxy/MCM-CeO_2	25	2.7	269	0.19
Doxy/MCM-41	25	2.8	553	0.54
Doxy2/MCM-41	40	2.8	235	0.26

All ceria-silica supports have large specific surface areas (500-700 m^2g^{-1}) and mesopore volumes ($V_{mesopore}$= 0.67–1.40 cm^3g^{-1}), necessary for obtaining high drug uptake values.

3.2. Doxycycline loading and characterization of hybrid materials

The incipient wetness impregnation method was chosen as the drug loading procedure because it is a fast and reliable procedure that minimizes the exposure of the unstable doxycycline molecules to light. Doxycycline was loaded onto the prepared ceria-based composites, as well as on pristine MCM-41 silica. A 25% drug weight fraction was used for all investigated carriers. As MCM-41 silica has a significantly larger specific surface value than the ceria-based composites, a 40 % doxycycline loading (wt.) MCM-41 hybrid material was also prepared.

The doxycycline presence in all hybrid samples was evidenced by FT-IR spectroscopy (Fig 4). The vibrations of the active pharmaceutical ingredient can be noticed in the range of 1700-1300 cm^{-1} in the spectra of hybrid samples, besides the characteristic vibrations of carrier: Si-O-Si (1225, 1090, 465 cm^{-1}) and Si-OH (966 cm^{-1}).

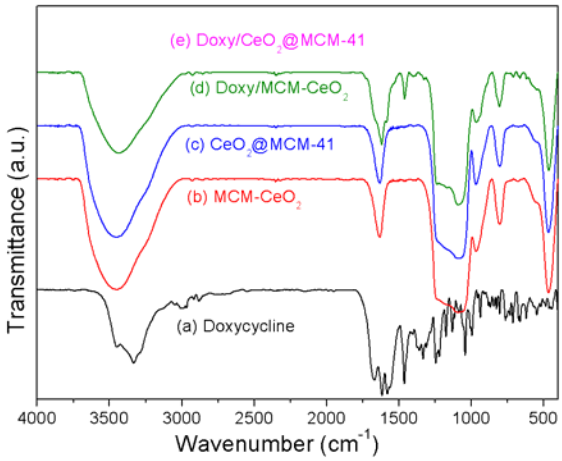

Fig. 4. FT-IR spectra of: doxycycline (a), MCM-CeO_2 (b), CeO_2@MCM-41, and doxycycline-based hybrid samples (d and e)

The small-angle and wide-angle XRD analyses of the doxycycline loaded materials (Fig. 5) indicate that the drug molecules are absorbed into the support mesochannels. The lack of doxycycline wide-angle diffraction peaks suggests that no crystalline drug phase is present, as expected if all drug molecules are adsorbed onto the carrier mesopores (Fig. 5). The order of the pore array is preserved after

the drug loading procedure, as the small-angle XRD patterns of the doxycycline-based hybrids are identical to the XRD patterns of the carriers (Fig. 5 inset).

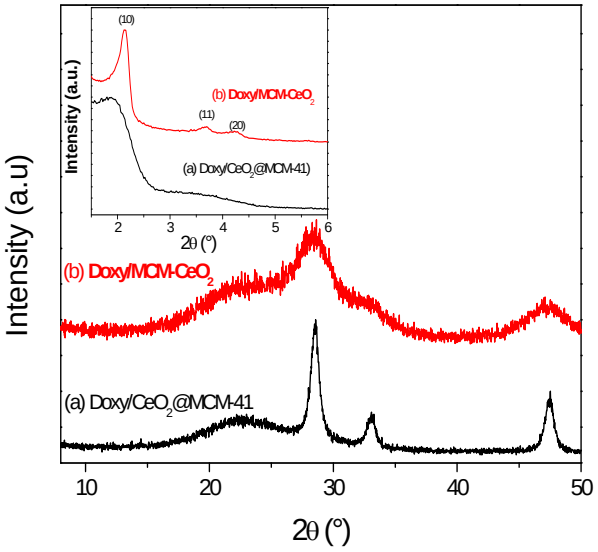

Fig. 5. Wide-angle XRD patterns of doxycycline loaded on ceria-based composite supports. Inset shows the small-angle XRD data for the same samples

The N_2 adsorption-desorption isotherms of the hybrid samples are type IV, characteristic to mesoporous materials (Fig. 6).

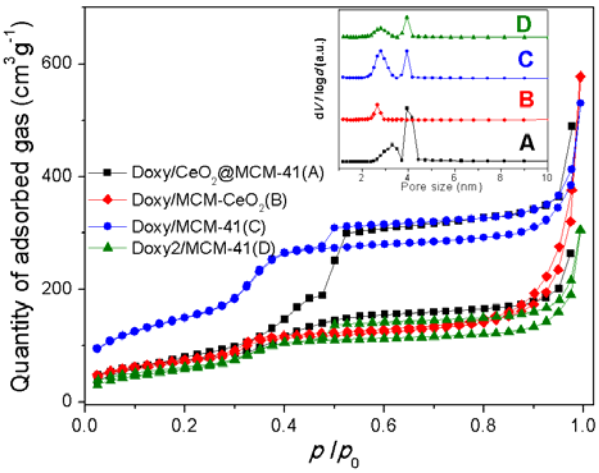

Fig. 6. N_2 adsorption-desorption isotherms of doxycycline-based hybrids. Inset shows the pore size distribution for the hybrid materials.

All samples contain a significant fraction of macropores. Moreover, the drug incorporation into mesochannels is supported by the reduced amount of physisorbed nitrogen volume in comparison with the corresponding supports, as well as the reduced pore volume and specific surface area values of doxycycline-based materials (Table 1). The drug adsorption process does not cause significant changes in the average pore size value, indicating weak interactions between the support and doxycycline molecules.

3.3. Doxycycline in vitro release

In vitro drug release experiments were performed at pH 5.5, close to the isoelectric pH of doxycycline, as the drug has the highest solution stability in these conditions [21].

Doxycycline dissolution at 37°C, pH 5.5 is almost complete after 15 minutes (Fig. 7D).

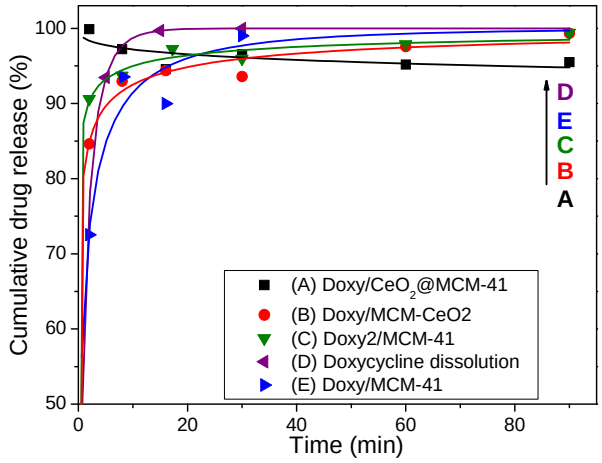

Fig. 7. Doxycycline cumulative release from the core-shell (A) and composite (B) ceria-silica supports, MCM-41 silica (C, E) and doxycycline dissolution (D) at 37°C, pH 5.5. Symbols indicate experimental data points, lines indicate data fitted with the Weibull model.

The drug release from MCM-CeO_2 or MCM-41 silica is slower than the dissolution of the pure antibiotic, with ~95% drug released after 40 minutes. Interestingly, a lower doxycycline weight fraction leads to a faster release profile (Fig. 8, E curve versus C curve), suggesting that the diffusion through the mesopores is the rate limiting step. The Doxy/MCM-CeO_2 hybrid material has the slowest release rate of the investigated materials (Fig.8B). In the case of the core-shell carrier (Fig. 8A), the most drug molecules are released in the first 2 minutes,

followed by a gradual decrease of drug concentration. This phenomenon could be explained by the adsorption of the active biological agent onto or close to the nanoparticle surface, leading to an almost instantaneously release, as the drug diffusion length into the mesopores is significantly reduced. The subsequent doxycycline concentration decrease might indicate drug readsorption into the support mesochannels.

Table 2

Weibull model parameters describing the experimental release data

Parameter	Doxy dissolution	Doxy/CeO_2@MCM-41	Doxy)/ MCM-CeO_2	Doxy/ MCM-41	Doxy2/ MCM-41
a	0.914	4.357	1.657	1.006	2.105
b	0.679	-0.086	0.194	0.389	0.153
R^2	1	0.9988	0.9986	0.9922	0.9994

The experimental release profiles were fitted using the Weibull model [21], a kinetic model based on the theory of percolation into fractal space. The cumulative release *F* is expressed as a two-parameter exponential function of time: $F(t)/F(\infty)= 1- exp(-at^b)$, where the *a* parameter is a measure of the release rate, while the *b* parameter indicates the ordering of the diffusion space, with values greater than ~0.69 indicating diffusion in Euclidian space and lower values signifying diffusion in fractal space [23]. The Weibull model parameters (Table 2) show that the release mechanism of the antibiotic molecules from silica and ceria-silica composites corresponds to diffusion in fractal space, as opposed to doxycycline dissolution (Euclidian space diffusion). Unlike in the case of SBA-15 mesoporous silica with larger pores [19], the increase in drug weight fraction leads to modifications of the diffusion mechanism, which can be explained by a decrease in drug diffusion and solvent counter diffusion rates as the free mesopore volume decreases. Regarding the ceria-silica mesoporous support MCM-CeO_2, it can be concluded that the doxycycline diffusion process is similar with the pristine MCM-41 silica carrier.

4. Conclusions

Two types of ceria-silica mesoporous materials were obtained by either two step procedure (“core-shell”) or one step method (“composite”). The ceria-silica nanomaterials present good porosity and good dispersion of the ceria nanoparticles inside and onto the silica mesochannels for the core-shell and composite materials, respectively. More ordered mesopore array was obtained for the composite MCM-CeO_2 synthesized by one step approach.

For the first time, we have shown that ceria-silica mesoporous materials can be used as matrices for the controlled delivery of doxycycline. In particular, the hybrid material containing 25% wt. therapeutic agent supported onto MCM-

CeO_2 composite material has the best drug release profile, combined with good porosity and high drug uptake values. This work therefore demonstrates a new application of ceria-silica mesoporous materials as carriers for drug delivery applications.

Acknowledgement

The Romanian project PCCA no. 131/2012 is gratefully acknowledged. The work of R. A. Mitran has been funded by the Sectoral Operational Programme Human Resources Development 2007–2013 of the Ministry of European Funds through the Financial Agreement POSDRU/159/1.5/S/132395.

R E F E R E N C E S

[1] *A. Trovarelli; F. Zamar; J. Llorca; C. d. Leitenburg; G. Dolcetti; J. T. Kiss,* Nanophase Fluorite-Structured CeO2–ZrO2Catalysts Prepared by High-Energy Mechanical Milling, Journal of Catalysis, **vol. 169** (2), 1997, pp. 490-502.

[2] *L. Jiang; M. Yao; B. Liu; Q. Li; R. Liu; H. Lv; S. Lu; C. Gong; B. Zou; T. Cui; B. Liu; G. Hu; T. Wågberg,* Controlled Synthesis of CeO2/Graphene Nanocomposites with Highly Enhanced Optical and Catalytic Properties, The Journal of Physical Chemistry C, **vol. 116** (21), 2012, pp. 11741-11745.

[3] *E. P. Murray; T. Tsai; S. A. Barnett,* A direct-methane fuel cell with a ceria-based anode, Nature, **vol. 400** (6745), 1999, pp. 649-651.

[4] *P. Jasinski; T. Suzuki; H. U. Anderson,* Nanocrystalline undoped ceria oxygen sensor, Sensors and Actuators B: Chemical, **vol. 95** (1–3), 2003, pp. 73-77.

[5] *J. R. Jurado,* Present several items on ceria-based ceramic electrolytes: synthesis, additive effects, reactivity and electrochemical behaviour, J Mater Sci, **vol. 36** (5), 2001, pp. 1133-1139.

[6] *J. Chen; S. Patil; S. Seal; J. F. McGinnis,* Rare earth nanoparticles prevent retinal degeneration induced by intracellular peroxides, Nat Nano, **vol. 1** (2), 2006, pp. 142-150.

[7] *A. S. Karakoti; N. A. Monteiro-Riviere; R. Aggarwal; J. P. Davis; R. J. Narayan; W. T. Self; J. McGinnis; S. Seal,* Nanoceria as antioxidant: Synthesis and biomedical applications, JOM, **vol. 60** (3), 2008, pp. 33-37.

[8] *M. Vallet-Regí; F. Balas; D. Arcos,* Mesoporous Materials for Drug Delivery, Angewandte Chemie International Edition, **vol. 46** (40), 2007, pp. 7548-7558.

[9] L. Băjenaru; S. Năstase; C. Matei; D. Berger, Studies On The Synthesis Of Mesoporous Aluminosilicates As Carries For Drug Delivery Systems, UPB Sci. Bull. Series B, vol. 73 (4), 2011, pp. 45 - 50.

[10] *R. C. S. Azevedo; R. G. Sousa; W. A. A. Macedo; E. M. B. Sousa,* Combining mesoporous silica–magnetite and thermally-sensitive polymers for applications in hyperthermia, J Sol-Gel Sci Technol, **vol. 72** (2), 2014, pp. 208-218.

[11] *R.-A. Mitran; D. Berger; L. Băjenaru; S. Năstase; C. Andronescu; C. Matei,* Azobenzene functionalized mesoporous AlMCM-41-type support for drug release applications, cent.eur.j.chem., **vol. 12** (7), 2014, pp. 788-795.

[12] *R. Liang; M. Wei; D. G. Evans; X. Duan,* Inorganic nanomaterials for bioimaging, targeted drug delivery and therapeutics, Chemical Communications, **vol.** 2014, pp.

[13] *R.-A. Mitran; S. Nastase; C. Matei; D. Berger,* Tailoring the dissolution rate enhancement of aminoglutethimide by functionalization of MCM-41 silica: a hydrogen bonding propensity approach, RSC Advances, **vol. 5** (4), 2015, pp. 2592-2601.
[14] *P. Borst; L. A. Grivell,* Mitochondrial ribosomes, FEBS Letters, **vol. 13** (2), 1971, pp. 73-88.
[15] *H. Iwasaki; H. Inoue; Y. Mitsuke; A. Badran; S. Ikegaya; T. Ueda,* Doxycycline induces apoptosis by way of caspase-3 activation with inhibition of matrix metalloproteinase in human T-lymphoblastic leukemia CCRF-CEM cells, Journal of Laboratory and Clinical Medicine, **vol. 140** (6), 2002, pp. 382-386.
[16] *W. C. M. Duivenvoorden; S. V. Popović; Š. Lhoták; E. Seidlitz; H. W. Hirte; R. G. Tozer; G. Singh,* Doxycycline Decreases Tumor Burden in a Bone Metastasis Model of Human Breast Cancer, Cancer Research, **vol. 62** (6), 2002, pp. 1588-1591.
[17] *N. Holmes, P. Charles* Safety and efficacy review of doxycycline. Clinical Medicine: Therapeutics. **1,** 2009 pp. 471–482.
[18] *R. A. Mitran; S. Nastase; C. Stan; A. I. Iorgu; C. Matei; D. Berger,* Doxycycline encapsulation studies into mesoporous SBA-15 silica type carriers and its in vitro release, 14th International Multidisciplinary Scientific GeoConference on Nano, Bio and Green: Technologies for Sustainable Future, **vol. 1** 2014, pp. 53-60.
[19] *R. A. Mitran; S. Nastase; L. Bajenaru; C. Matei; D. Berger,* Mesostructured Aluminosilicates As Carriers For Doxycycline-Based Drug Delivery Systems, 14th International Multidisciplinary Scientific GeoConference on Nano, Bio and Green: Technologies for Sustainable Future, **vol. 1** 2014, pp. 113-120.
[20] *A. H. Janssen; A. J. Koster; K. P. de Jong,* On the Shape of the Mesopores in Zeolite Y:□ A Three-Dimensional Transmission Electron Microscopy Study Combined with Texture Analysis, The Journal of Physical Chemistry B, **vol. 106** (46), 2002, pp. 11905-11909.
[21] *R. Injac; V. Djordjevic-Milic; B. Srdjenovic,* Thermostability Testing and Degradation Profiles of Doxycycline in Bulk, Tablets, and Capsules by HPLC, Journal of Chromatographic Science, **vol. 45** (9), 2007, pp. 623-628.
[22] *K. Kosmidis; P. Argyrakis; P. Macheras,* Fractal kinetics in drug release from finite fractal matrices, The Journal of Chemical Physics, **vol. 119** (12), 2003, pp. 6373-6377.
[23] *V. Papadopoulou; K. Kosmidis; M. Vlachou; P. Macheras,* On the use of the Weibull function for the discernment of drug release mechanisms, International Journal of Pharmaceutics, **vol. 309** (1–2), 2006, pp. 44-50.